Tropical Journal of Pharmaceutical Research June 2026; 25 (6): 761-772
ISSN: 1596-5996 (print); 1596-9827 (electronic)

Available online at http://www.tjpr.org
https://dx.doi.org/10.4314/tjpr.v25i6.2

Original Research Article

Development of mucoadhesive solid lipid nanoparticles for enhanced oral bioavailability and antimalarial efficacy of artemether/lumefantrine

Emmanuel Chekwube Ossai[1]*, Patience Chinenye Ugwuoke[1], Chukwuemeka Ome Agbom[1], Edith Ogochukwu Ossai[2], Momoh A Mumuni[3], Christian Tobechukwu Ezike[1], Christian Chukwuemeka Mbah[4]

[1]Department of Biochemistry, University of Nigeria, Nsukka, [2]Department of Pediatrics, University of Nigeria Teaching Hospital, Enugu, [3]Department of Pharmaceutics, University of Nigeria, Nsukka, [4]Department of Pharmaceutical Technology and Industrial Pharmacy, University of Nigeria, Nsukka, Enugu State, Nigeria

For correspondence: **Email: emmanuel.ossai@unn.edu.ng; **Tel:** +2347038514389*

Sent for review: 22 January 2026 *Revised accepted: 18 June 2026*

Abstract

Purpose: *To report the development of mucoadhesive solid lipid nanoparticles (SLNs) to enhance oral bioavailability and antimalarial efficacy of artemether and lumefantrine.*
Methods: *The SLNs were prepared via hot emulsion–ultrasonication using a lipid matrix composed of dika fat (Irvingia gabonensis) and Phospholipon® 90H. Chitosan coating was applied to confer mucoadhesive properties and prolong gastrointestinal residence time. Fourier transform infrared (FTIR) spectroscopy and differential scanning calorimetry (DSC) were employed to determine the drug-excipient interaction and thermal properties of the nanoparticles, respectively. Antimalarial properties of the formulated nanoparticles were carried out in vivo using Plasmodium berghei-infected Wistar albino mice.*
Results: *The SLNs, formulated as individual and co-drug-loaded systems, achieved high encapsulation efficiencies (> 99 % for artemether; > 92 % for lumefantrine). Co-loading improved drug release compared to single-drug SLNs (artemether: 86.2 vs. 58.7 %; lumefantrine: 74.8 vs. 63.8 % over 6 – 8 h). The nanoparticles were spherical, with mean diameters 91.3 – 140.1 nm and polydispersity indices < 0.42. Fourier transform infrared spectroscopy and DSC analyses confirmed drug–excipient compatibility and stable incorporation of both drugs within the lipid matrix. In vivo evaluation in Plasmodium berghei-infected Wistar albino mice revealed a dose-dependent, statistically significant ($p < 0.05$) reduction in parasitemia for the SLN formulations compared to control.*
Conclusion: *Chitosan-coated SLNs offer a promising platform for oral delivery of artemether-lumefantrine, with potential to overcome current limitations in bioavailability and therapeutic consistency in malaria treatment.*

Keywords: *Antimalarial efficacy, Artemether, Bioavailability, Chitosan coating, Drug release, Encapsulation efficiency, Lumefantrine, Malaria, Solid lipid nanoparticles*

Tropical Journal of Pharmaceutical Research is indexed by Scopus, Chemical Abstracts, Embase, Index Copernicus, EBSCO, African Index Medicus, JournalSeek, Directory of Open Access Journals (DOAJ), African Journal Online, Bioline International, Open-J-Gate and Pharmacy Abstracts

INTRODUCTION

Malaria continues to pose a threat despite improvements in vector control and diagnostics because drug-resistant strains are emerging, underscoring the need for better treatment approaches. The main treatment for malaria is still chemotherapy, the effectiveness that have been hampered by widespread resistance to traditional medications [1]. Because of their strong and quick antimalarial action, artemisinin-based combination therapies (ACTs), specifically, artemether–lumefantrine, have become the gold standard for treating uncomplicated P. falciparum malaria [2]. This is due to the synergistic effects of longer-acting lumefantrine and fast-acting artemether [3].

Artemether-lumefantrine has a low and variable oral bioavailability due to its significant presystemic metabolism and poor aqueous solubility, which hinders its therapeutic potential despite its clinical utility [4]. This drawback can be mitigated by incorporating the drugs into solid lipid nanoparticles (SLNs) as lipid-based formulations [5]. The SLNs are usually formed using phosphatidyl derivatives to change the lipid matrix or mixing different lipid types to create less ordered crystalline structures [6], and coating them with chitosan would improve their mucoadhesive qualities and by extension, drug absorption and gastrointestinal retention.

The integration of chitosan-coated SLNs using dika fat and phospholipid-based matrices for dual drug delivery of artemether and lumefantrine remains a critical knowledge gap despite the large number of studies on SLNs and ACTs. This study sought to create and describe chitosan-coated SLNs co-loaded with artemether and lumefantrine using a lipid matrix made of dika (plant-based) fat and Phospholipon® 90H, addressing the limitations of conventional oral ACTs. The SLNs were prepared by ultrasonication and assessed for particle size, encapsulation efficiency, in vitro release, morphology, thermal stability, and drug–excipient interactions. The antimalarial efficacy of the formulations was evaluated using *Plasmodium berghei*-infected Wistar albino mice.

EXPERIMENTAL

Extraction of Dika Fat from *Irvingia gabonensis*

Soxhlet extraction of dika fat from seeds of *I. gabonensis* was done with n-hexane. The hexane was evaporated at room temperature, and the fat was depolymerized using boiling water and ethyl acetate. The crude fat was purified via passage through a charcoal–bentonite column (2:1 w/w) at 100 °C (10 g fat:1 g adsorbent) and stored at 4 °C until use.

Preparation of lipid matrix

A lipid matrix was formulated by melting dika fat and Phospholipon® 90H (P90H) at a 2:1 ratio, as described by Onyishi *et al* [7]. Briefly, 40 g of P90H was mixed with 80 g of dika wax in a crucible and melted at 80 °C using a water bath (Zenith Lab, Jiangsu, China). The mixture was stirred and allowed to cool at room temperature to obtain a solid lipid matrix.

Preparation of Solid Lipid Nanoparticles (SLNs)

The SLNs were prepared via ultrasonication, following Agbo *et al* [8]. The lipid matrix (DW: P90H, 5 g) was melted at 60 °C, and the drug (artemether, lumefantrine, or both) was incorporated. Aqueous surfactant solution (containing 2 % PVA, 0.1 % sorbic acid, 2 % sorbitol, and 2 % chitosan) preheated to 60 °C was added. The total volume was adjusted to 100 mL with distilled water. The emulsion was sonicated for 10 min at 60 °C using a probe ultrasonicator (Athena Technology, Mumbai, India; 71 W, 1:1 pulse ratio), cooled to room temperature, and stored at 4 °C. The composition of the drugs in the batch formulations is presented in Table 1.

Table 1: Summary of the composition of the SLN formulations

Batch	Artemether (mg)	Lumefantrine (mg)
A_1	50	-
A_2	100	-
A_3	200	-
B_1	-	100
B_2	-	200
B_3	-	400
C_1	50	100
C_2	100	200
C_3	200	400
C_0	-	-

Characterization of SLNs

Drug encapsulation efficiency

Drug encapsulation efficiency (EE %) was determined according to Agbo *et al* [8]. Briefly, 2 mL of SLN was diluted with 2 mL of water, cooled at 4 °C for 5 min, and centrifuged (13,000 rpm, 40 min). Artemether (after derivatization) and lumefantrine concentrations in the supernatant were analyzed at 254 nm and

342 nm, respectively. Artemether was derivatized by reacting 1 mL of supernatant with 25 mL of 1 N HCl and heating at 80 °C for 30 min, followed by dilution to 100 mL. Encapsulation efficiency (EE %) was calculated using Eq 1.

EE (%) = {(Wa-Ws)/Wa}100 ….. (1)

where *W*a is the initial drug amount and *W*s is the drug quantity in the supernatant.

In vitro drug release

Drug release from SLNs was assessed using dialysis membrane (MWCO 12,400 Da, pore size 2.4 nm), pre-soaked in simulated intestinal fluid (SIF, pH 7.4). Three mL of formulation was sealed in 5-cm dialysis bags and suspended in 250 mL of SIF at 37 °C with stirring (70 rpm). At 30-min intervals, 5 mL samples were withdrawn and replaced with fresh medium. Drug content was analyzed spectrophotometrically (254 nm for artemether after derivatization; 342 nm for lumefantrine).

Morphological characterization

The morphology of SLNs was evaluated using scanning electron microscopy (SEM; JSM-6400, Joel, USA). Samples were diluted, air-dried on SEM stubs, and gold-coated before imaging.

Particle size and polydispersity index

A DLS scan was used to determine particle size and polydispersity index (PDI) of the formulations. A drop of SLNs was dispersed in deionized water and measured at 25 °C and a 90° scattering angle.

Fourier-Transform Infrared (FTIR) Spectroscopy

An FTIR analysis was conducted to assess interactions between drugs and excipients. Samples were mixed with KBr, compressed into pellets, and scanned over 4000 – 400 cm^{-1}.

Differential Scanning Calorimetry (DSC)

Thermal analysis was conducted on samples (~5 mg), sealed in aluminum pans and heated from 20 – 350 °C at 5 °C/min temperature increment.

In vivo antimalarial evaluation

Antimalarial activity was evaluated following a curative protocol using adult albino Wistar mice (n = 40) infected with *Plasmodium berghei* (ANKA strain). After 6 days of infection, animals were grouped (n = 10) and treated orally from day 7 to day 9 with:

Group 1: 10 mg/kg of C_1

Group 2: 10 mg/kg of C_2

Group 3: 0.2 mL of C_0 (blank)

Group 4: 10 mg/kg of standard ACT

Parasitemia was assessed on day 10 by Giemsa-stained thin smears. Percentage parasitemia (P) and reduction (R) were calculated using Eq 2 and 3.

$P (\%) = (N_{RBC}/T_{RBC})100$ …….. (2)

$R (\%) = (M_{pre}-M_{post})/M_{pre}\}100$ …….. (3)

Where N_{RCB} is the number of infected RBC, T_{RBC} is the total number of RBC, while M_{pre} and M_{post} represent mean pretreatment and posttreatment parasitemia, respectively.

The animals were handled following the ethical guidelines on the use of laboratory animals established by the Faculty of Biological Sciences' Ethics and Biosafety Committee, University of Nigeria, Nsukka, with project license number: UNN/FBS/24/SS.9367, and in compliance with the International Standard for the use of laboratory animals [9].

Hematological analysis

Blood samples collected before and after treatment were analyzed for hematological indices (WBC, RBC, Hb, PCV) using an automated hematology analyzer (Sysmex XS 500i, Hyogo, Japan).

Histopathological examination

One animal from each group was euthanized on day 10. Liver and kidney tissues were fixed in 10 % formalin, dehydrated with graded ethanol, cleared in chloroform, embedded in paraffin, sectioned (5 – 6 µm), stained with hematoxylin and eosin (H&E), and examined using a photomicroscope (D-MOTICAM 580, USA).

Statistical analysis

All experiments were performed in triplicate. Data were analyzed using ANOVA and Student's *t*-test in SPSS (IBM Corp., USA). Significance was set at $p < 0.05$. Results are presented as mean ± SD.

RESULTS

Encapsulation Efficiency

Table 2 showed that all formulations demonstrated high encapsulation efficiencies, with values increasing proportionally with the drug concentration. Artemether-loaded SLNs exhibited encapsulation efficiencies ranging from 99.62 % to 99.85 %, while lumefantrine-loaded SLNs showed values between 92.12 % and 96.23 %. For co-loaded SLNs, artemether encapsulation efficiency ranged from 99.16 % to 99.86%, and lumefantrine from 92.52 % to 96.82 % (Table 2).

Table 2: Encapsulation efficiency of artemether- and lumefantrine-loaded solid lipid nanoparticles

Formulations	Encapsulation Efficiency (%)
A_1	99.62 ± 0.17
A_2	99.61 ± 0.14
A_3	99.85 ± 0.18
B_1	92.12 ± 0.19
B_2	94.94 ± 0.16
B_3	96.23 ± 0.11
AC_1	99.16 ± 0.15
AC_2	99.72 ± 0.13
AC_3	99.86 ± 0.17
BC_1	92.52 ± 0.10
BC_2	94.65 ± 0.16
BC_3	96.82 ± 0.13

Values are expressed as mean ± standard deviation (SD) of triplicate determinations. **Key:** A_1, A_2, A_3: SLNs containing 50, 100, and 200 mg of artemether, respectively. B_1, B_2, B_3: SLNs containing 100, 200, and 400 mg of lumefantrine, respectively. AC_1, AC_2, AC_3: For artemether encapsulation efficiency in SLNs co-loaded with 50, 100, and 200 mg of artemether, respectively, and 100, 200, and 400 mg of lumefantrine, respectively. BC_1, BC_2, BC_3: For lumefantrine encapsulation efficiency in SLNs co-loaded with the same artemether and lumefantrine combinations as in the ACs above.

In vitro drug release studies of Artemether/Lumefantrine-loaded SLNs

Figures 1 to 3 revealed a biphasic release pattern, with an initial burst release followed by sustained drug release. Quantitatively, after 6 h in simulated intestinal fluid, artemether released from single-drug-loaded SLNs was 58.75, 39.75, and 25.74 % for formulations A_1, A_2, and A_3, respectively. Conversely, in co-loaded SLNs, artemether release was significantly enhanced: 86.20, 70.57, and 40.78 % (AC_1, AC_2, and AC_3, respectively; Figures 1 a to c). Whereas, for lumefantrine single-drug-loaded SLNs (Figures 2a to 2c), the drug release at 8 h was 63.75 %, 48.38, and 24.19 % (Formulations B_1, B_2, and B_3, respectively). However, in co-loaded SLNs (Figures 2a to c), lumefantrine release was also significantly enhanced: 74.75 % (BC_1), 61.86 % (BC_2), and 29.75 % (BC_3). Figures 3 a to c show the release profiles for artemether and lumefantrine in the combinational formulations, and artemether consistently showed a faster release profile than lumefantrine across all co-loaded formulations (Figures 1 to 3).

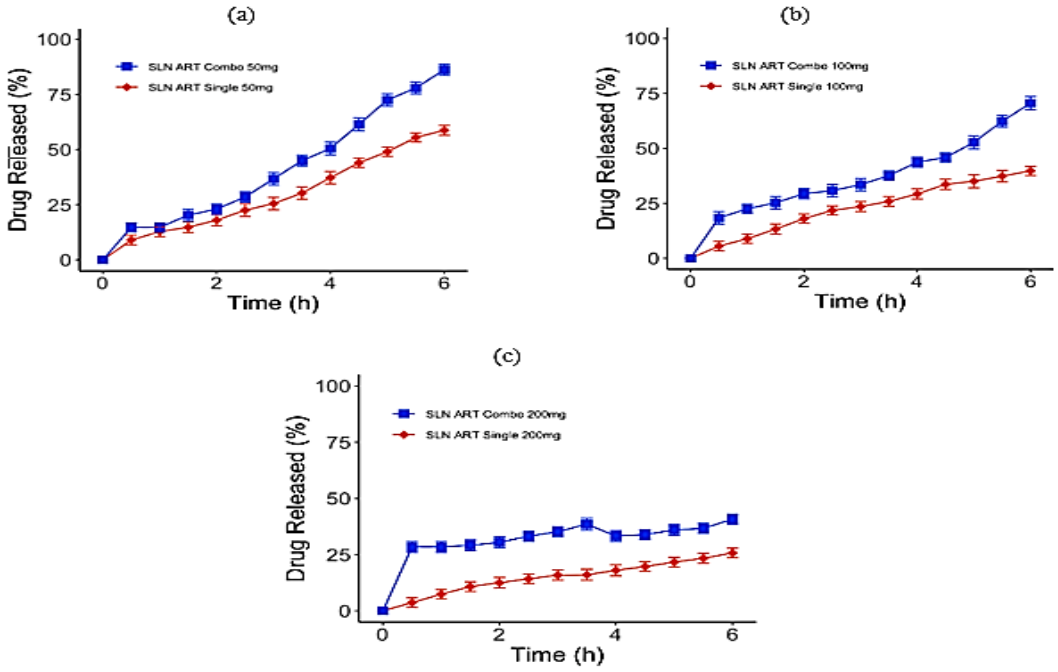

Figure 1: Release profile of artemether in formulations (a) A_1 vs AC_1, (b) A_2 vs AC_2, (c) A_3 vs AC_3

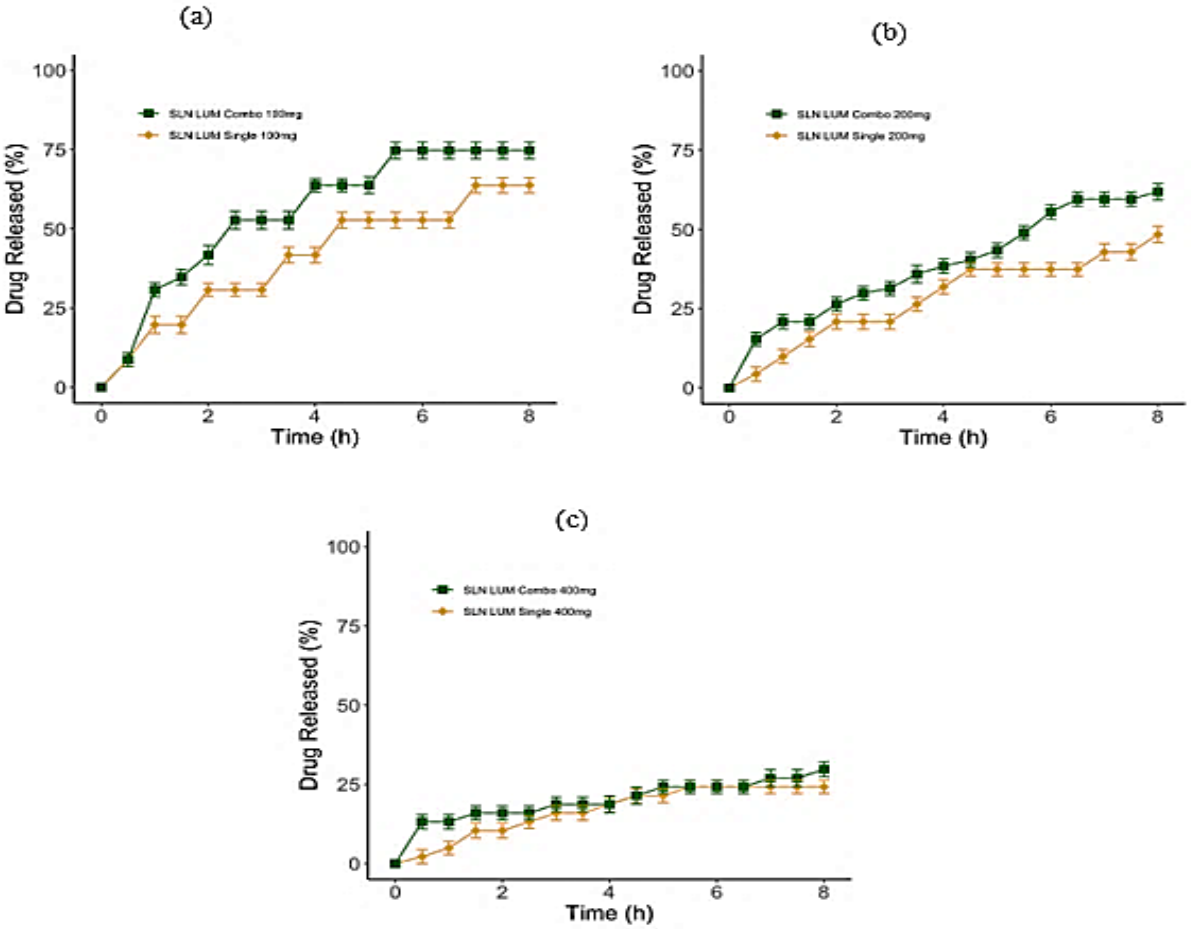

Figure 2: Release profile of lumefantrine in formulations (a) B_1 vs BC_1, (b) B_2 vs BC_2, (c)B_3 vs BC_3

Particle morphology and size

The morphology results show that the SLNs exhibited smooth, spherical, and non-porous structures (Figure 4). Particle size analysis (Figure 4 d) indicated mean diameters of 140.1 ± 1.67 nm for C_0 (unloaded SLN), 101.6 ± 1.72 nm for C_1 (SLN co-loaded with 50 mg of artemether and 100 mg of lumefantrine), and 91.27 ± 1.65 nm for C_2 (SLN co-loaded with 100 mg of artemether and 200 mg of lumefantrine). The corresponding polydispersity index (PDI) values were 0.364 ± 0.15 for C_0, 0.368 ± 0.11 for C_1, and 0.418 ± 0.21 for C_2 (Figure 4).

FTIR analysis

FTIR spectra of artemether (Figure 5 a) showed three distinguishing peaks of C–H stretching vibrations at 2937.1, 2877.5, and 2847.7 cm^{-1}. For lumefantrine, major peaks were observed at 3391.9 cm^{-1} for OH stretching vibrations, 2926.0 and 2870.1 cm^{-1} for C–H stretching vibrations, 1632.6 cm^{-1} for aromatic C=C stretching vibrations; whereas those of P90H showed a characteristic broad peak at 3362.1 cm^{-1} for OH stretching vibrations, two distinguished peaks of C-H stretching at 2918.5 and 2891.4 cm^{-1}, and C=O stretching vibrations at 1736.9 cm^{-1}. The FTIR spectra of dika fat showed characteristic peaks at 3444.1 cm^{-1} for OH stretching, 2918.5 and 2851.4 cm^{-1} for C-H stretching, and 1740.7 cm^{-1} for C=O vibrations. For the co-drug-loaded SLN formulations, FTIR spectra of C_1 and C_2 showed similar peaks at 3350.9 cm^{-1} for OH stretching, 2922.2 and 2851.4 cm^{-1} for C–H stretching vibrations, 1744.4 cm^{-1} for C=O vibrations, and 1636.3 cm^{-1} for aromatic C=C stretching vibrations.

Thermal analysis

The DSC thermogram of artemether (Figure 5(b)) exhibited a sharp endothermic peak at 86.57 °C, while lumefantrine showed a sharp peak at 127.5 °C. Phospholipon® 90H displayed an endothermic peak at 122.5 °C, and dika fat exhibited a broad endothermic peak at 57.5 °C. For the formulated SLNs, broad endothermic peaks were observed at 112.5 °C for both C_1 and C_2 (Figure 5).

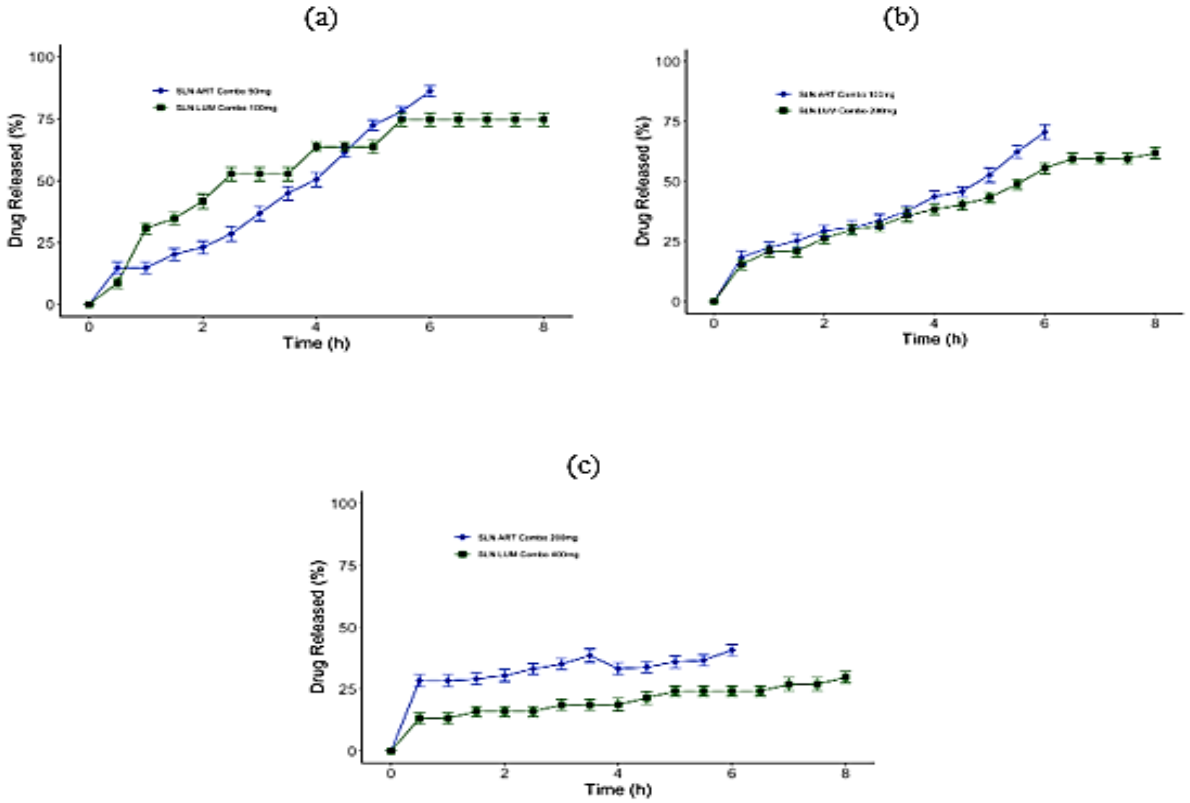

Figure 3: Release profile of ACT formulations in (a) AC_1 vs BC_1, (b) AC_2 vs BC_2, (c) AC_3 vs BC_3

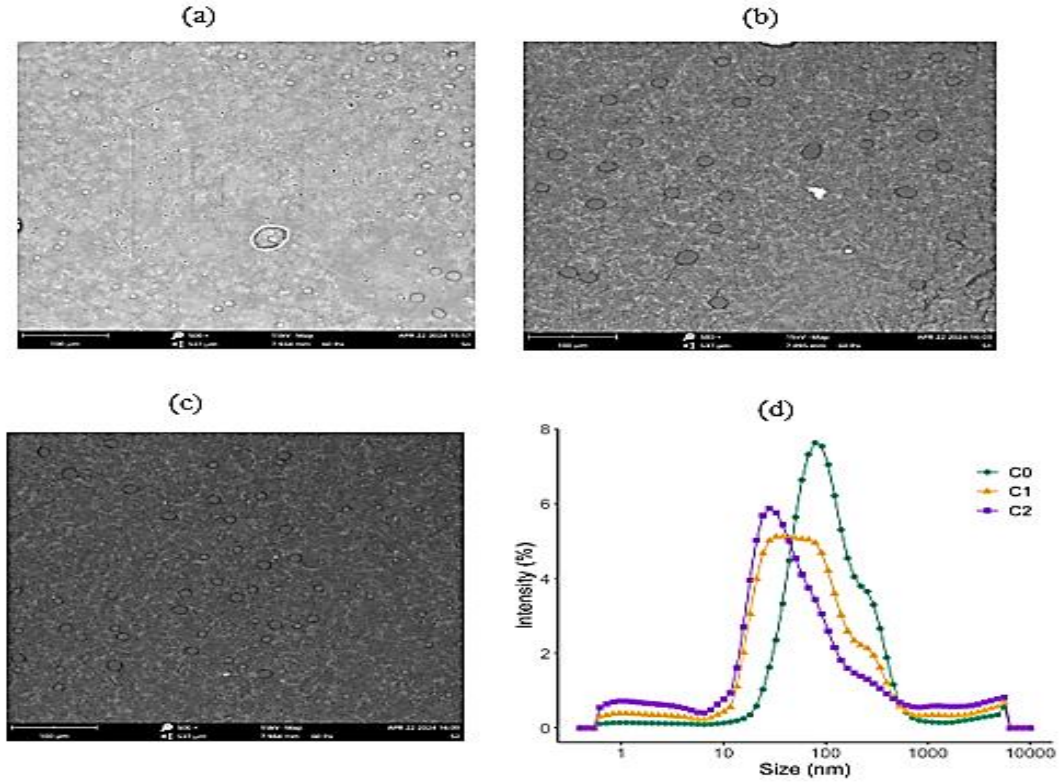

Figure 4: Morphology and particle size characterizations illustrating SEM photomicrography of (a) C_0; unloaded SLN, (b) C_1; SLN co-loaded with 50 mg of ART and 100 mg of LUM, (c) C_2; SLN co-loaded with 100 mg ART and 200 mg LUM, (d) Size distribution of unloaded SLN (C_0), SLN co-loaded with 50 mg of ART and 100 mg of LUM (C_1) SLN co-loaded with 100 mg ART and 200 mg LUM (C_2)

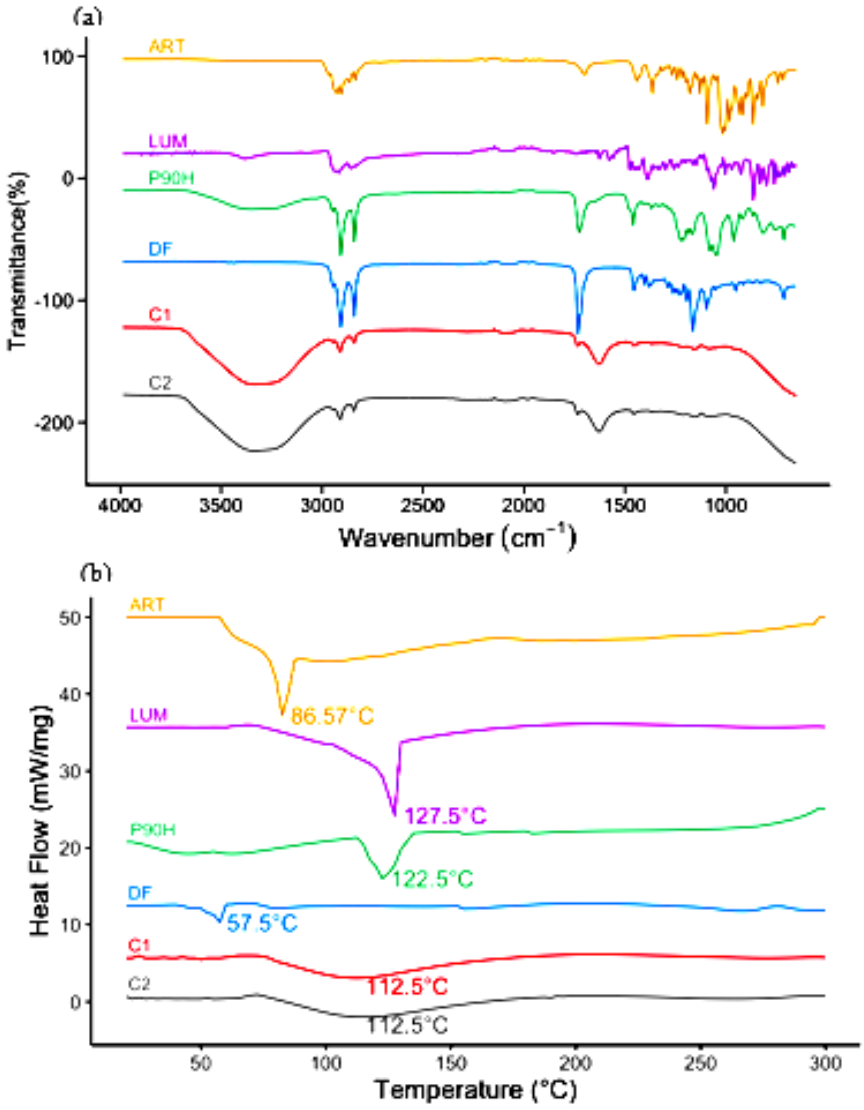

Figure 5: Biophysical characterization of SLN formulations showing (a) FTIR spectra and (b) DSC photomicrographs of artemether (ART), lumefantrine (LUM), P90H, Dika fat (DF), C1 (SLN loaded with 50 mg of ART and 100 mg of LUM), and C2 (SLN loaded with 100 mg of ART and 200 mg of LUM)

In vivo antimalarial evaluation

Results show that on day 4 of treatment, the placebo-treated group (C_0) exhibited an 11.96 % increase in parasitemia (Figure 6 a). In contrast, groups treated with SLNs containing 50:100 mg of artemether/lumefantrine (C_1) and 100:200 mg of artemether/lumefantrine (C_2) demonstrated reductions in parasitemia of 38.42% and 52.22 %, respectively. The reference group treated with a marketed ACT sample (MS) showed a 41.86 % reduction in parasitemia. These findings indicate that the SLN formulations exhibited a dose-dependent reduction in parasitemia levels. The co-drug-loaded SLN (C_2) demonstrated significantly enhanced antimalarial activity compared to a commercial artemisinin-based combination therapy (ACT) reference.

Effect of formulated SLNs on weight of animals

Throughout the treatment period, no significant changes in body weight were observed in any of the treatment groups (Figure 6 b), indicating that the SLN formulations did not adversely affect the growth or general health status of the animals (Figure 6).

Effect of formulations on hematological indices

Animal treatment with C_1, C_2, and MS resulted in non-significant ($p > 0.05$) increases in RBC, Hb, and PCV levels (Figure 7). Conversely, a non-significant decrease ($p > 0.05$) in these parameters was observed in the C_0 (unloaded SLN) group. WBC counts increased non-

significantly in groups treated with C_0, C_1, and C_2, whereas a non-significant decrease in WBC was noted in the group treated with the MS. In all, animals treated with drug-loaded SLNs (C_1 and C_2) and the commercial ACT exhibited increased RBC, PCV, and Hb levels, whereas the placebo group (unloaded SLNs, C_0) showed decline in these indices (Figure 7).

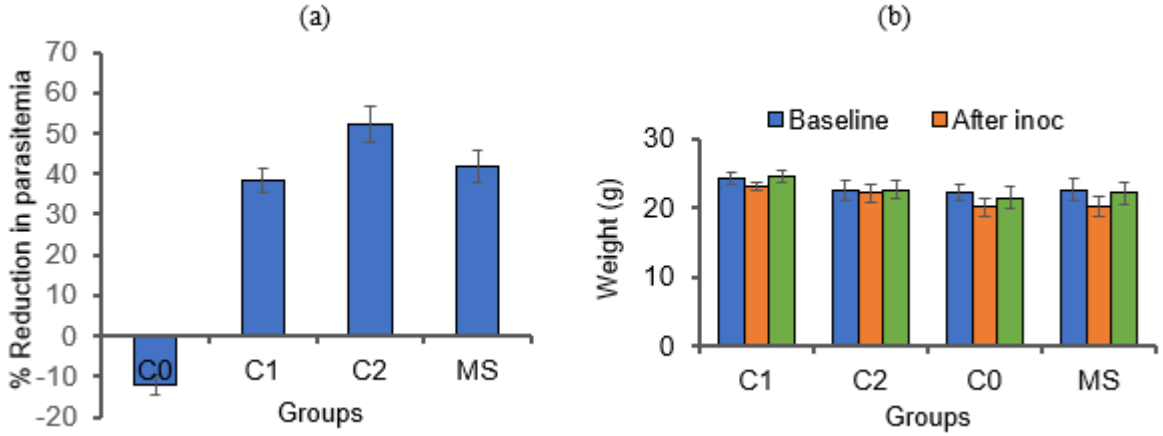

Figure 6: Effect of treatment on (a) parasitemia reduction and (b) weight changes across groups

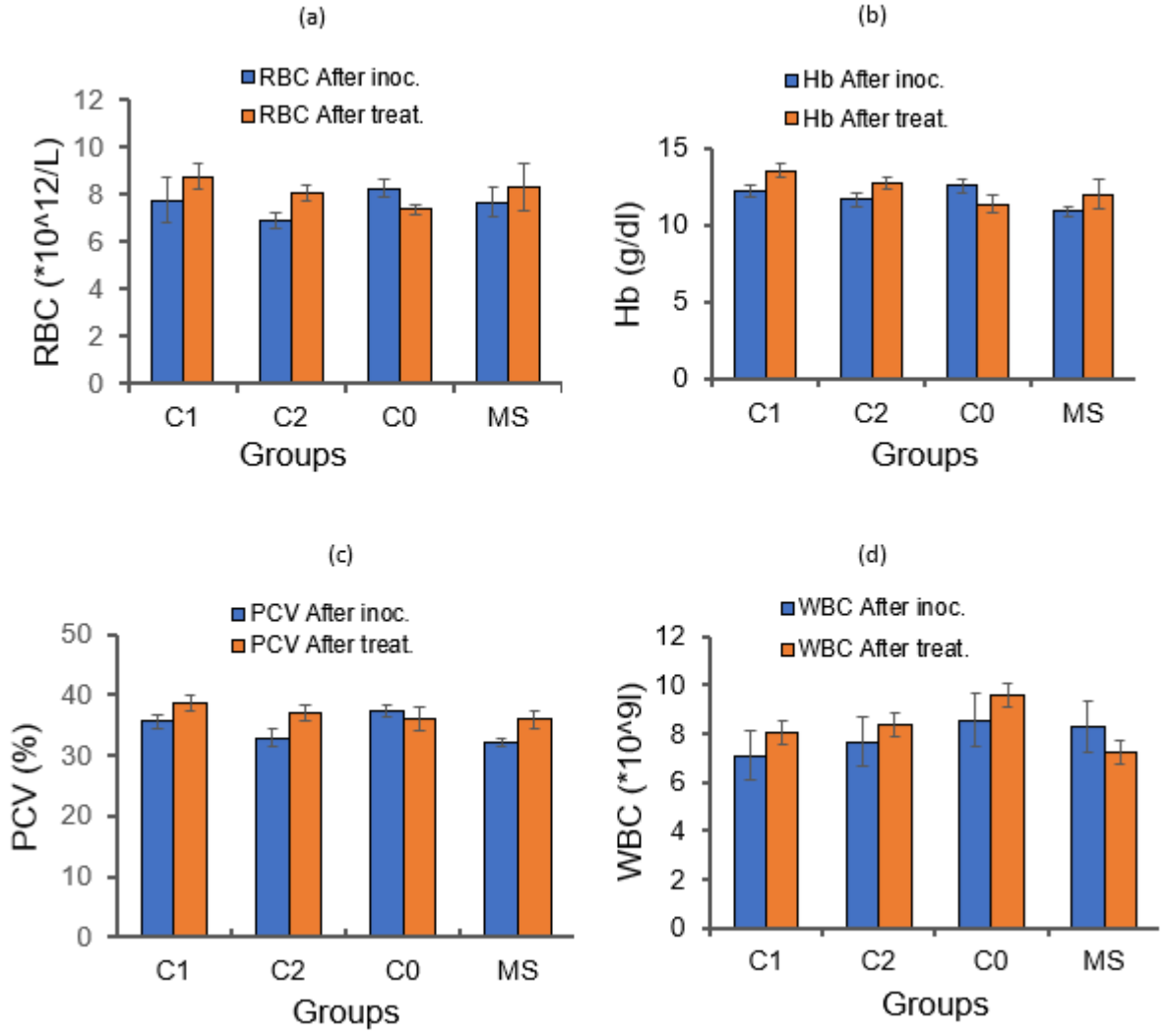

Figure 7: Effect of treatment on (a) RBC, (b) Hb, (c) PCV and (d) WBC of animals

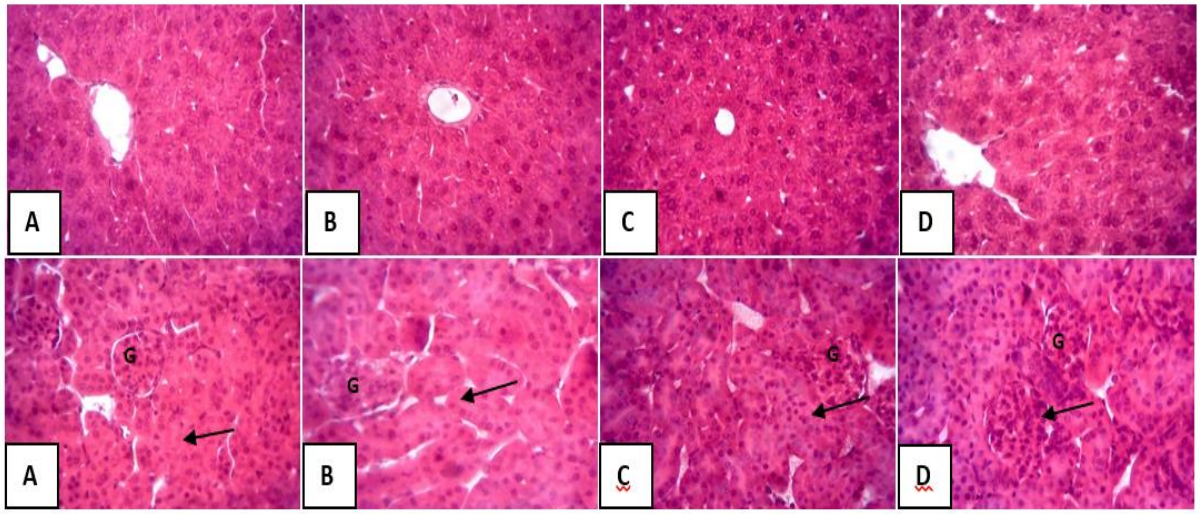

Figure 8: Photomicrographs of liver (top panel) and kidney (bottom panel) tissues from group treated with C_1 (SLN co-loaded with 50 mg of ART and 100 mg of LUM, A), C_2 (SLN co-loaded with 100 mg ART and 200 mg LUM, B), MS (ACT market sample, C), C_0 (unloaded SLN, D)

Histopathological studies on formulated SLNs

Histological assessment of the liver sections (Figure 8, top panel) revealed normal hepatocytes with intact cell membranes across all treatment groups. Liver sections showed well-preserved hepatocytes radiating from the central vein, with intact portal triads. Mild mononuclear cell infiltration was observed only in the placebo group (C_0). Similarly, kidney sections (bottom panel) showed normal histological architecture of the glomeruli and renal tubules with no sign of toxicities in all groups examined (Figure 8).

DISCUSSION

The effectiveness of solid lipid nanoparticles (SLNs) as drug delivery systems (DDS) is determined by the drug encapsulation efficiency (% EE) as a crucial factor. In this study, exceptionally high % EE values were obtained, especially with increase in drug concentrations, which are in line with reports that higher drug concentrations can improve encapsulation [10] and imply that different drug concentrations in the formulations may have caused minor variations in % EE.

The biphasic pattern of the *in vitro* release profiles of artemether and lumefantrine from the formulations is typical of SLNs and is generally attributed to the rapid desorption of surface-associated drug molecules during the initial phase, followed by a slower diffusion-controlled release of the drug entrapped within the lipid [11]. Notably, the consistently faster release rate of artemether more than lumefantrine across all co-loaded formulations may be attributed to the markedly higher lipophilicity of lumefantrine (log P 9.19) relative to artemether (log P 3.53), which likely promotes stronger partitioning of lumefantrine into the hydrophobic lipid core and consequently retards its diffusion [12]. The more compact molecular structure of artemether may also facilitate its faster diffusion. Such staggered release is advantageous in artemether–lumefantrine combination therapy, enabling rapid parasite clearance by artemether followed by sustained suppression and prevention of recrudescence by lumefantrine [3]. In the present study, the slower release at higher drug loading could be due to enhanced hydrophobic interactions within the lipid matrix, leading to increased encapsulation efficiency and reduced drug diffusion. Similar trends were reported for carvedilol SLNs [13]. Based on the favorable release characteristics, particularly the minimal burst effect and balanced biphasic release, formulations C_1 and C_2 were selected for further physicochemical characterization and *in vivo* evaluation.

The smooth, spherical, and non-porous morphology of the formulations, as revealed by SEM, is consistent with SLNs prepared from chemically polydisperse lipid matrices and can be attributed to the blend of dika fat and P90H used in the present formulation. This is so since highly pure lipids often yield cuboid particles, whereas mixed-lipid systems favor spherical morphology, which is advantageous for drug loading and distribution, offering high stability, increased surface area, and protection of the encapsulated drug for controlled release [14].

The inverse relationship of particle size with increasing drug concentration is attributed to stronger hydrophobic interactions between artemether–lumefantrine and the lipid matrix, leading to a more compact SLN core, and to potential hydrogen bonding between the hydroxyl groups of lumefantrine and surfactant molecules, thereby reducing the interfacial tension and facilitating particle size reduction [15]. Similar particle size reductions with higher drug loading were reported for magnesium lithospermate B-loaded SLNs [16].

Spectrophotometric analysis showed that co-drug-loaded SLN formulations (C_1 and C_2) maintained the characteristic peaks of the individual components, with minor attenuation of some drug-specific peaks, potentially due to peak overlapping associated with hydrogen bonding or ionic interactions within the formulation components [3]. The absence of new peaks indicates no significant chemical interactions or new bond formation between the drugs and the lipid excipients. The disappearance of certain minor peaks from the drugs' spectra upon encapsulation likely reflects physical embedding and electrostatic interactions among oppositely charged functional groups rather than chemical alteration.

The sharp endothermic melting peaks of pure artemether and lumefantrine are consistent with literature values [17], confirming their crystalline purity, so also the melting transitions for P90H and dika fat [18]. Importantly, co-drug-loaded SLN formulations (C_1 and C_2) exhibited broad endothermic peaks at temperatures in between the values for those of the lipid components, with no detectable crystalline drug melting peaks. This disappearance of drug-specific melting transitions in the formulations suggests molecular dispersion of artemether and lumefantrine within the lipid matrix, likely in amorphous or solubilized states, and is known to enhance dissolution rates and bioavailability by increasing drug wettability and reducing crystallinity [19]. Overall, the FTIR and DSC analyses confirm the successful incorporation of artemether and lumefantrine into the SLNs without chemical incompatibility, and their transition into a more bioavailable physical state within the lipid matrix.

The therapeutic efficacy of artemether/lumefantrine-loaded SLNs evaluated in mice infected with *Plasmodium berghei* improved with increased drug-loading, and is attributed to factors including enhanced drug solubilization within the lipid matrix, mucoadhesive interactions imparted by surface-bound chitosan enhancing intestinal retention and absorption, and protection from enzymatic degradation during presystemic transit. Furthermore, the sustained-release nature of the SLNs could mitigate fluctuations in plasma drug levels, maintaining therapeutic concentrations over an extended period. These findings align with previous reports on dihydroartemisinin, chloroquine, and dihydroartemisinin/lumefantrine [14].

The developed SLN formulations exhibited an excellent safety profile, as evidenced by the absence of significant changes in body weight, hematological parameters, and histopathology of liver and kidney tissues, underscoring their systemic biocompatibility and suitability for oral antimalarial delivery.

The decrease in the hematological parameters (RBC, PCV, and Hb levels) observed in the C_0 group likely resulted from progressive parasitemia, causing intravascular hemolysis, increased clearance of infected erythrocytes, and disrupted erythropoiesis [20]. The improvements in hematological parameters following treatment with C_1, C_2, and ACT are attributed to parasitemia reduction and potential stimulatory effects of the formulations on erythropoiesis, aligning with literature report [14]. Although these increases were not statistically significant by day 4, longer observation periods may reveal more pronounced effects.

The mild mononuclear cell infiltration of hepatocytes of the placebo group (C_0), unlike in the treatment groups, as revealed by the histopathological examination, likely reflects parasitemia-induced inflammation. The normal histological architectures of hepatic and renal tissues of the treated groups support the biocompatibility of the SLN formulations, although further long-term toxicity studies are recommended to validate these preliminary findings.

CONCLUSION

A dika fat–phospholipon 90H lipid matrix has been successfully used to formulate chitosan-coated solid lipid nanoparticles (SLNs) co-loaded with lumefantrine and artemether. Drug–lipid compatibility was confirmed by FTIR and DSC, and the nanoparticles demonstrate a favorable size distribution, high encapsulation efficiency, and biphasic drug release. Without having an adverse effect on body weight, hematological indices, or organ histology, SLNs showed dose-dependent antimalarial activity *in vivo*, with higher doses reducing parasitemia more than a

reference ACT. These results demonstrate the potential of chitosan-coated SLNs with a plant-based lipid template as secure, efficient oral delivery systems for poorly soluble antimalarial drugs. For clinical translation, future research should examine the pharmacokinetics, stability, and scale-up.

DECLARATIONS

Acknowledgement/Funding

This work was supported by the Federal Government of Nigeria through the Tertiary Education Trust Fund (TETFund)-National Research Fund (NRF), Grant number TETF/ES/DR&D-CE/NRF2023/SETI/HSW/00245/VOL.1

Ethical approval

The ethical approval for the use of laboratory animals was issued by the Faculty of Biological Sciences' Ethics and Biosafety Committee, University of Nigeria, Nsukka, with project license number: UNN/FBS/24/SS.9367.

Availability of data and materials

The datasets used and/or analyzed during the current study are available from the corresponding author on reasonable request.

Conflict of Interest

No conflict of interest is associated with this work.

Use of Artificial intelligence/Large language models

The authors confirm that AI-based tools were used solely for language editing and manuscript polishing purposes (e.g., grammar, phrasing, and clarity). No AI tools were used to generate content, interpret data, or influence study design, results, or conclusions. All intellectual contributions, study analyses, and interpretations reported in the manuscript are the original work of the authors.

Contribution of authors

We declare that this work was done by the authors named in this article and all liabilities pertaining to claims relating to the content of this article will be borne by the authors.

REFERENCES

1. *Kilonzi M, Minzi O, Mutagonda R, Sasi P, Kamuhabwa A, Aklillu E. Comparison of malaria treatment outcomes of generic and innovator's anti-malarial drugs containing artemether-lumefantrine combination in the management of uncomplicated malaria amongst Tanzanian children. Malar J 2019; 18(1): 1-9.*
2. *World Health Organization. World Malaria Report 2024. Geneva: WHO; 2024. Available from: https://www.who.int/teams/global-malaria-programme/reports/world-malaria-report-2024.*
3. *Akpa PA, Ugwuoke JA, Attama AA, Ugwu CN, Ezeibe EN, Momoh MA, et al. Improved antimalarial activity of caprol-based nanostructured lipid carriers encapsulating artemether-lumefantrine for oral administration. Afr Health Sci 2020; 20(4): 1679-1697. doi: 10.4314/ahs.v20i4.20.*
4. *Pawar S, Shende P. Dual drug delivery of cyclodextrin cross-linked artemether and lumefantrine nanosponges for synergistic action using 23 full factorial designs. Colloids Surf A Physicochem Eng Asp 2020; 602: 125049.*
5. *Nnamani PO, Ugwu AA, Ibezim EC, Kenechukwu FC, Akpa PA, Ogbonna JN, et al. Sustained-release liquisolid compact tablets containing artemether-lumefantrine as alternate-day regimen for malaria treatment to improve patient compliance. Int J Nanomed 2016; 11: 6365-6378. doi: 10.2147/IJN.S92755.*
6. *Gordillo-Galeano A, Mora-Huertas CE. Solid lipid nanoparticles and nanostructured lipid carriers: A review emphasizing particle structure and drug release. Eur J Pharm Biopharm 2018; 133: 285–308.*
7. *Onyishi IV, Chime SA, Attama AA. Evaluation of excipient potentials of Irvingia wombolu fats and Moringa oil in rifampicin-loaded lipospheres: in vitro-in vivo characterisation. J Drug Deliv Sci Technol 2014; 24(4): 404–412.*
8. *Agbo CP, Ugwuanyi TC, Ugwuoke WI, McConville C, Attama AA, Ofokansi KC. Intranasal artesunate-loaded nanostructured lipid carriers: A convenient alternative to parenteral formulations for the treatment of severe and cerebral malaria. J Control Release 2021; 334: 224–236.*
9. *National Research Council. Guide for the care and use of laboratory animals, National Academies Press. Washington, DC; 2010.*
10. *Subramaniam B, Siddik ZH, Nagoor NH. Optimization of nanostructured lipid carriers: understanding the types, designs, and parameters in the process of formulations. J Nanopart Res 2020; 22(6): 1–29.*
11. *Kraisit P, Hirun N, Mahadlek J, Limmatvapirat S. Fluconazole-loaded solid lipid nanoparticles (SLNs) as a potential carrier for buccal drug delivery of oral candidiasis treatment using the Box-Behnken design. J Drug Deliv Sci Technol 2021; 63: 102437.*
12. *Volpe-Zanutto F, Ferreira LT, Permana AD, Kirkby M, Paredes AJ, Vora LK, et al. Artemether and lumefantrine*

dissolving microneedle patches with improved pharmacokinetic performance and antimalarial efficacy in mice infected with Plasmodium yoelii. J Control Rel 2021; 333: 298-315. doi: 10.1016/j.jconrel.2021.03.036.

13. *El-Say KM, Hosny KM. Optimization of carvedilol solid lipid nanoparticles: An approach to control the release and enhance the oral bioavailability in rabbits. PLoS One 2018; 13(8): e0200955.*
14. *Odera PA, Otieno G, Onyango JO, Owuor JJ, Oloo FA, Ongas M, et al. Nanoparticle-based formulation of dihydroartemisinin-lumefantrine duo-drugs: Preclinical Evaluation and enhanced antimalarial efficacy in a mouse model. Heliyon 2024; 10(6): e26868.*
15. *Rawal SU, Patel MM. Lipid nanoparticulate systems: Modern versatile drug carriers. In: Lipid Nanocarriers for Drug Targeting 2018; 49–138.*
16. *Kang X, Chen H, Li S, Jie L, Hu J, Wang X, et al. Magnesium lithospermate B-loaded PEGylated solid lipid nanoparticles for improved oral bioavailability. Colloids Surf B Biointerfaces 2018; 161: 597–605.*
17. *Garg A, Tomar DS, Bhalala K, Wahajuddin M. Development and investigation of Artemether loaded binary solid lipid nanoparticles: Physicochemical characterization and in-situ single-pass intestinal permeability. J Drug Deliv Sci Technol 2020; 60: 102072.*
18. *Ugwu CE, Oraeluno JN, Eze KC, Ezenma CO, Nwankwo AO. PEGylated aceclofenac solid lipid microparticles homolipid-based solidified reverse micellar solutions for drug delivery. Heliyon 2022; 8(4): e09234.*
19. *Shah P, Chavda K, Vyas B, Patel S. Formulation development of linagliptin solid lipid nanoparticles for oral bioavailability enhancement: role of P-gp inhibition. Drug Deliv Transl Res 2021; 11(3): 1166–1185.*
20. *Diederich L, Suvorava T, Sansone R, Keller TCS 4th, Barbarino F, Sutton TR, et al. On the effects of reactive oxygen species and nitric oxide on red blood cell deformability. Front Physiol 2018; 9: 332. doi: 10.3389/fphys.2018.00332.*